

The Seyfert AGN RX J0136.9-3510 and the Spectral State of Super Eddington Accretion Flows

Chichuan Jin, Chris Done, Martin Ward, Marek Gierliński, James Mullaney
Department of Physics, University of Durham, South Road, Durham, DH1 3LE, UK

31 October 2018

ABSTRACT

We have carried out a survey of long 50ks XMM-Newton observations of a sample of bright, variable AGN. We found a distinctive energy dependence of the variability in RXJ0136.9-3510 where the fractional variability increases from 0.3 to 2 keV, and then remains constant. This is in sharp contrast to other AGN where the X-ray variability is either flat or falling with energy, sometimes with a peak at ~ 2 keV superimposed on the overall trend. Intriguingly these unusual characteristics of the variability are shared by one other AGN, namely RE J1034+396, which is so far unique showing a significant X-ray Quasi-Periodic Oscillation (QPO). In addition the broad band spectrum of RXJ0136.9-3510 is also remarkably similar to that of RE J1034+396, being dominated by a huge soft excess in the EUV-soft X-ray bandpass. The bolometric luminosity of RX J0136.9-3510 gives an Eddington ratio of about 2.7 for a black hole mass (from the H beta line width) of $7.9 \times 10^7 M_{\odot}$. This mass is about a factor of 50 higher than that of RE J1034+396, making any QPO undetectable in this length of observation. Nonetheless, its X-ray spectral and variability similarities suggest that RE J1034+396 is simply the closest representative of a new class of AGN spectra, representing the most extreme mass accretion rates.

Key words: accretion, Eddington ratio, SED, active-galaxies: nuclei

1 INTRODUCTION

Active galactic nuclei (AGN) are powered by gas accreting onto the central super-massive black hole. As such their intrinsic spectra are determined simply by the mass and spin of the black hole, together with the mass accretion rate, although their observational appearance is also affected by absorption. The discovery that the black hole mass scales with the host galaxy bulge properties (Gebhardt et al. 2000; Magorrian et al. 1998) presented a means to classify the bewildering variety of unabsorbed AGN spectra in terms of two of these three intrinsic properties. It was found that different optical spectral types clearly correlated with black hole mass and mass accretion rate, with the Narrow-line Seyfert 1 galaxies (NLS1s: defined as $H\beta$ emission line FWHMs less than 2000 km/s and $[OIII]/H\beta$ flux ratios less than 3.0 Goodrich 1989) as examples of lower mass black holes accreting at higher Eddington ratio than the typical broad line Seyfert 1s (BLS1s), which in turn had higher Eddington ratio/lower black hole masses than the LINERSs (e.g. Osterbrock & Pogge 1985; Boller, Brandt & Fink 1996; Boroson 2002; Mathur 2000; Bian et al. 2008; Winter et al. 2009).

NLS1s are intrinsically very luminous in the EUV/soft

X-ray bandpass, comprising over half the AGN found in the softest X-ray selected surveys (Puchnarewicz et al. 1992; Grupe et al. 1996; Edelson et al. 1999). This strong ionising flux results in intense permitted optical Fe II emission lines from the broad line region and high ionisation species often referred to as coronal lines (Wills et al. 1999; Kuraszewicz et al. 2000; Ghosh et al. 2004; Mullaney & Ward 2008). Other observed characteristics include rapid X-ray variability (Leighly 1999a; Boller, Brandt & Fink 1996) and steeper soft X-ray spectra than those of BLS1s (Leighly 1999b; Brandt, Mathur & Elvis 1997). Taken together these distinctive properties have led to them being considered as the scaled up counterparts of the most luminous accretion states seen in stellar mass black hole binary (BHB) systems ie. those having “high” and “very high” states (Pounds, Done & Osborne 1995; Middleton, Done & Gierliński 2007).

This link with the stellar mass black hole systems was strengthened by the first detection of an X-ray QPO in the NLS1 RE J1034+396 (Gierliński et al. 2008) as QPOs are commonly seen in the BHB systems (e.g. Remillard & McClintock 2006). While there are multiple different types of QPO in the BHB (high fre-

quency QPO, low frequency QPO, plus some others seen only in GRS1915+105: e.g. Remillard & McClintock 2006; Morgan, Remillard & Greiner 1997), they are all generally most prominent in the ‘very high state’. Simple scaling from BHB then predicts that QPO’s should be common amongst NLS1 as a class due to their high mass accretion rate. Nonetheless, RE J1034+396 is extreme even amongst NLS1 (see below), and it may be that its so far unique QPO detection is due more to its unusual properties than to any simple scaling from the known QPO’s in BHB.

We first summarise the properties of RE J1034+396, in order to provide the context for our study of RX J0136.9-3510, which is reported in this paper. The most obvious unusual feature of RE J1034+396 is its broad band spectral energy distribution (SED). This exhibits a peak in the far UV which connects smoothly onto the steep soft X-ray spectrum. These components form a huge “soft X-ray excess” with respect to the $\Gamma \sim 2.2$ X-ray tail which dominates above ~ 2 keV (Puchnarewicz et al. 1995; Casebeer, Leighly & Baron 2006; Middleton, Done & Gierliński 2007; Middleton et al. 2009). The energy dependence of this variability is also very different to that commonly seen in other AGN. The fractional variability amplitude (as measured by root mean square, hereafter *rms*) rises steeply to ~ 2 keV and then levels off. This is most likely due to the presence of two separate components in the X-ray spectrum, with the variability being associated with the X-ray tail, whilst the soft excess component remains more or less constant (Middleton et al. 2009). This situation contrasts with the flat or falling *rms* spectra seen in other AGN, sometimes with a peak at ~ 2 keV superimposed on this (Vaughan et al. 2003; Vaughan et al. 2004; Fabian et al. 2004; Gierliński & Done 2006; Ponti et al. 2006; Petrucci et al. 2007; Larsson et al. 2008), which makes it more likely that the apparent soft excess in these objects is due instead to a single spectral component distorted by reflection and/or absorption (Crummy et al. 2006; Gierliński & Done 2006).

In this paper we make use of the unusual energy dependence of the X-ray variability in RE J1034+396 to search for potentially similar objects. A survey of all long ($\gtrsim 50$ ks) XMM-Newton observations of bright and variable AGN yielded a similar *rms* shape only in one object RX J0136.9-3510 (2MASS J0136544-350952). This AGN also has a similar broadband spectrum to RE J1034+396, suggesting that they may form a subclass of the highest mass accretion rate AGN.

2 SOURCE SELECTION

We searched the *XMM-Newton Master Log & Public Archive* for pointed observations with exposure times in the PN instrument of ≥ 50000 s in “subject_category” “AGN, QSOs, BL-Lacs and XRB”. This resulted in 115 observations available at the time of our study (November 2008). We further refined this criteria to include only those objects with PN count rates of $\gtrsim 1.0$ counts/s, to include only bright sources for which the variability can be well determined.

We also searched the *XMM-Newton Serendipitous Source Catalogue (2XMMi Version)* for serendipitous bright AGN detected in similarly long exposures, by setting

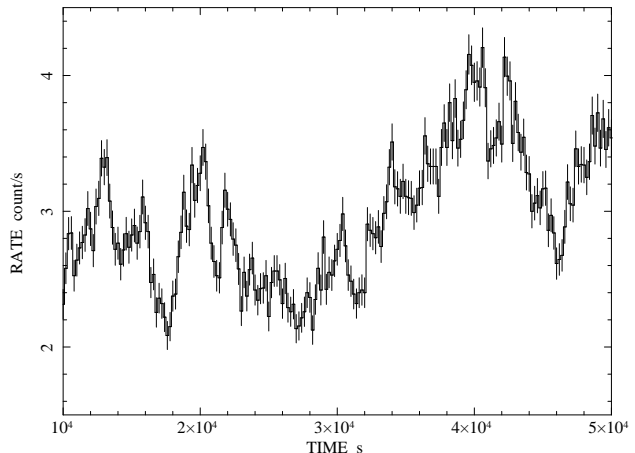


Figure 1. Background subtracted lightcurve of RX J0136.9-3510 binned on 200 s. The exposure start time (UTC) is 2005-12-14 20:45:30, but the first 10 ks was excluded due to the high background contamination.

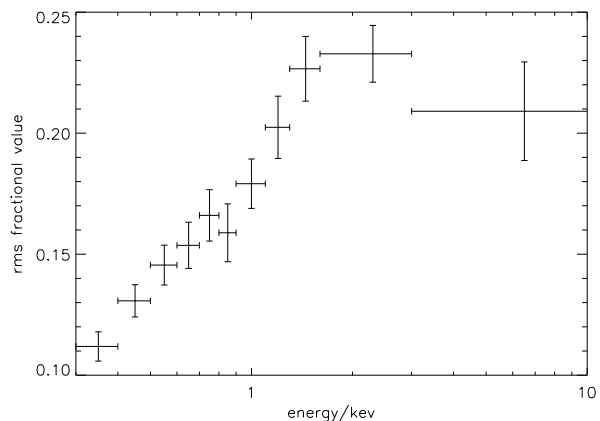


Figure 2. The *rms* spectrum corresponding to Figure 1, the binning time is 2000s.

$\text{pn_s_flux} \geq 10^{-12}$ erg cm $^{-2}$ s $^{-1}$ and $\text{pn_ontime} \geq 50000$ s. This yielded 29 observations.

We then combined these two samples to give a total of 68 individual sources. For each dataset we calculated the fractional variability amplitude using `lcstats` in `xronos` 5.21. This is defined as the root mean square of the intrinsic (corrected for error bars) variance about the lightcurve mean, σ^2 , normalised to this mean, I . Only sources which are strongly and significantly variable can provide constraints on the energy dependence of the variability, so we select only sources for which the *rms* is ≥ 0.1 at more than 3 sigma significance (determined from the uncertainty on the *rms*, which relates to the χ^2 distribution as the variance is a sum of squares, see e.g. Done et al. (1990)). This filtering leaves 19 AGNs.

We then excluded 2 known BL Lac objects (PKS2155-304 and 0716+714) since their X-ray variability is thought to be due to jet related processes. For the two observations of NGC 4051, one (0157560101) only has an exposure time of 49917 s, while the other (0109141401) does not have the

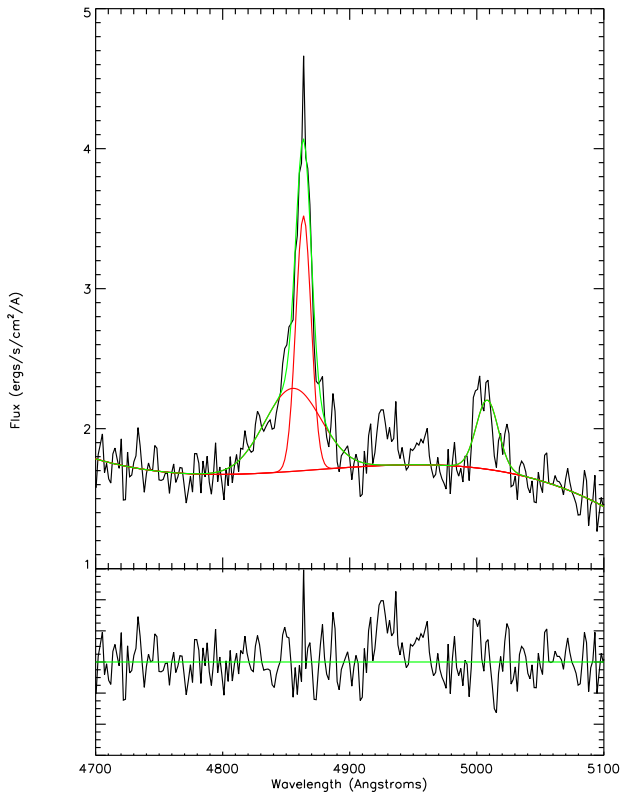


Figure 3. The optical spectrum of RX J0136.9-3510, including the H β emission line fitting. The data is from Grupe D. and we show this figure with his permission.

pn_time value in the catalog, so they were formerly excluded by the filtering. However, since NGC 4051 is a well known, bright, NLS1 and our study is not a statistical study, we still included these two observations. This inclusion should not affect our general conclusions. We also included the famous Seyfert 2 AGN, MCG-5-23-16 (0302850201), although its *rms* variability is only 0.073. This gives us a total of 19 AGNs for subsequent study, with one or more selected observations for each of them.

For each of these datasets we calculated the fractional variability amplitude as a function of energy using the method of Gierliński & Done (2006). This showed the standard range of *rms* spectral shapes. Only RX J0136.9-3510 (0303340101) displayed the very different type of *rms* spectrum associated with the QPO AGN, RE J1034+396, in which the fractional amplitude rises as a function of energy, then remains high. Having identified this unusual AGN, we investigate its properties in more detail below.

3 RX J0136-3510: LIGHTCURVE AND RMS SPECTRUM

The lightcurve and *rms* spectrum are extracted from the X-ray data (0.3-10 keV), using SAS7.1.0 and xronos5.21. We use regions with radius of 70'', 40'' and 40'' for pn, MOS1 and MOS2, respectively. No significant pile-up is seen from the SAS command `epatplot` so no central region was excluded. There are high background flares during the first 10000 s, so we exclude these data, resulting in ~ 40000 s

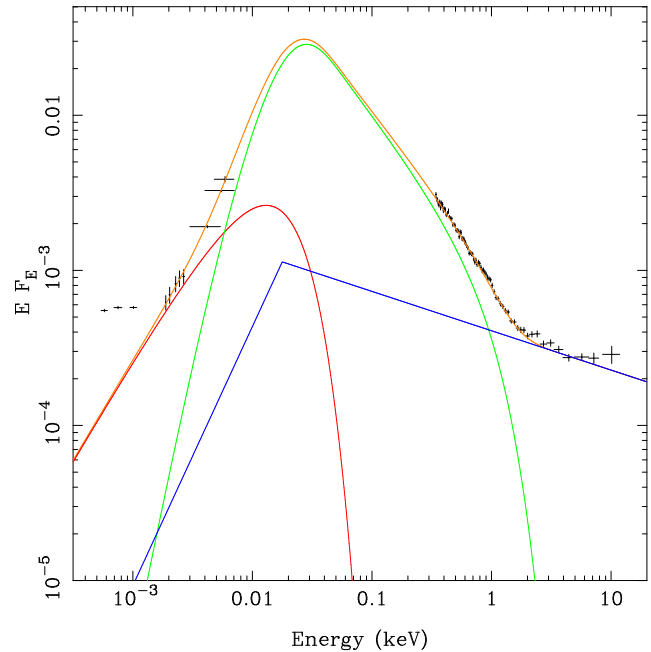


Figure 4. RX J0136.9-3510 unfolded spectrum. All data points from different wave bands are included in this figure, though the infrared points are not included in the model fitting. The model spectrum without galactic extinction and dust reddening is also generated and superposed on the source spectrum, with red representing redshifted disk component, green representing *compTT* and blue representing *bknpower*. The orange line shows the total model spectrum.

(with background count rate < 0.4 counts/s) for the *rms* spectrum generation. Figure 1 shows the resultant total lightcurve (PN, MOS1 and MOS2), binned on 200 s. The source shows strong variability (also seen by Ghosh et al. 2009, in preparation), with the *rms* fractional variation being 0.13. However, there is no obvious QPO, and a power spectral analysis shows no peaks above even 1σ significance using the method of Vaughan (2005).

We rebin the lightcurve on 2000 s in order to provide enough count statistics to calculate the fractional variability as a function of energy. Fig. 2 shows that this *rms* rises steeply from 0.3 keV to ~ 2 keV, then flattens off. The weak decrease from 2-10 keV is not significant as the low count rate means their are large uncertainties on the last point. We also calculated the *rms* spectra from 200 s binning, but this is not significantly different.

4 BLACK HOLE MASS ESTIMATION

The optical spectrum has an *FeII*/H β flux ratio of ~ 8.3 (Grupe et al. 1999), compared to the ~ 1 average for NLS1s (Véron-Cetty, Véron & Goncalves 2001), making RX J0136.9-3510 an unusual NLS1 (Ghosh et al. 2004). We use the optical spectrum shown in Fig 3 (D. Grupe, private communication) to estimate the black hole mass. The H β line width is used as a proxy for this (see Woo & Urry 2002 and references therein) from

$$M_{BH} = 4.817 \times \left[\frac{\lambda L_{\lambda}(5100\text{\AA})}{10^{44} \text{ergs}^{-1}} \right]^{0.7} FWHM^2 \quad (1)$$

Table 1. The best-fit parameters in our model for the optical to X-ray broad band SED.

constant 2	T_{disk} (eV)	kT_e (keV)	τ	N_{comp}	Γ_{pow}	N_{pow}	$\chi^2_{\nu}/\text{d.o.f}$
$0.92^{+0.10}_{-0.10}$	$7.93^{+0.28}_{-0.31}$	$0.28^{+0.03}_{-0.02}$	$12.17^{+0.72}_{-0.75}$	$10.64^{+2.37}_{-1.73}$	$2.28^{+0.07}_{-0.08}$	$1.12^{+0.55}_{-0.37}$	475/493

Comparing this method for a sample of AGN with reverberation mapping, the rms difference is about 0.5 dex (Woo & Urry 2002). The flux at $\lambda = 5100\text{\AA}$ from the optical spectrum is $\sim 1.5 \times 10^{-16} \text{ erg cm}^{-2} \text{ s}^{-1}$. The luminosity distance is $D_L = 1455.2$ Mpc for $z = 0.289$ assuming $H_0 = 72$ km Mpc $^{-1}$, $\Omega_M = 0.27$, and $\Omega_{vac} = 0.73$.

Estimating the FWHM of the line is not straightforward as the $H\beta$ line profile is complex. There is clearly also a component from the extended narrow line region (NLR). This should be similar to the profile of the [OIII] emission line. So Grupe et al. (1999) use a template constructed from the [OIII] $\lambda 5007$ line to represent the narrow component, together with a broader Gaussian component, with FWHM=1320 km/s, to reconstruct the $H\beta$ line. This gives a black hole mass estimate of $1.3 \times 10^7 M_{\odot}$.

However, the optical spectrum plainly has limited signal-to-noise, and the [OIII] 5007 line is probably contaminated by FeII emission as it should be in 3:1 ratio with the (unobserved) [OIII] line at 4959 \AA . Hence we perform our own best fit of the $H\beta$ line profile with a gaussian of width 870 km/s for the narrow line component, see Figure 3. This gives a FWHM for the broad component of 3200 ± 2600 km s $^{-1}$, with a (not significant) blueshift of -370 ± 1100 km s $^{-1}$. Using our new value for the FWHM, the resultant black hole mass is $7.85 \times 10^7 M_{\odot}$.

Even with this lower black hole mass, this AGN is still probably $\sim 10\times$ more massive than the QPO AGN, RE J1034+396, (with the previous mass estimate being $\sim 50\times$ larger). Thus any similar QPO in RX J0136.9-3510 would be on timescales $10\text{-}50\times$ larger, requiring a much longer X-ray observation in order to detect it.

5 BROAD BAND SED ANALYSIS AND EDDINGTON RATIO

We use the standard products to obtain the XMM-Newton X-ray (PN) spectra and optical/UV (OM) photometry. We then combine these with selected continuum points from the (non-simultaneous) optical spectrum (D. Grupe, private communication) using `FLX2XSP` to incorporate these into the same format as the XMM-Newton data. We likewise include the J,H and K near infrared flux points from 2MASS, and perform all spectral fitting using `xspec11.3.2`.

We follow the approach of Vasudevan & Fabian (2009) in modelling the broadband SED, using `diskpn` to model an accretion disc extending down to the last stable orbit around a non-spinning black hole. However, our source is at $z = 0.289$ so we modify the `diskpn` code to incorporate the redshift dependence. The normalisation of the `diskpn` model is $(M^2 \cos i)/(D_{kpc}^2 \beta^4)$ where M is the mass in solar units, D_{kpc} is the distance in kpc, and the cosine of the inclination and colour temperature correction ($\cos i$ and β , respectively) are both set to unity following Vasudevan & Fabian (2009). We start at the highest estimated black hole mass

in Section 4, which gives a `diskpn` normalization of 2910, and fix this in the spectral fitting. Compton scattering of these disc photons can be approximated by a broken power law (`bknpower`), with index of $\Gamma = 0.33$ below a break at $3kT_{disk}$. We then added a low temperature Comptonisation component to model the soft excess, using `comptt`, with seed photons set to the disc temperature. We assume that these intrinsic components are absorbed by both gas and dust in our Galaxy, and so fix this parameter to the the Galactic HI column¹ (`wabs`) value of $N_H = 0.0208 \times 10^{22} \text{ cm}^{-2}$. The reddening (`redden`) is linked to this assuming a $E(B-V) = 1.74 \times 10^{-22} N_H$ (Spitzer 1978). Since the optical data were not simultaneous with the UV and X-ray data, we allow for long time-scale variation as a constant offset in normalisation between the XMM-Newton data and the optical spectrum. We exclude the infrared data points from our spectral fitting, since the model we use describes the intrinsic emission from the accretion flow whereas the infrared emission is likely due to reprocessing of the UV emission by dust in the host galaxy, plus a possible contribution from intrinsic starlight. The resultant best-fit parameters are given in Table 1.

Figure 4 shows the rebinned data (black), with the optical flux corrected for their best fit normalisation of $\sim 0.92\times$ that of the XMM-Newton UV and X-ray spectra, and all datapoints are corrected for absorption/reddening. This model is a good description of the overall shape of the optical/UV/X-ray spectrum and gives a bolometric (0.001-100 keV) flux of $1.1 \times 10^{-10} \text{ erg cm}^{-2} \text{ s}^{-1}$, corresponding to a bolometric luminosity of $2.7 \times 10^{46} \text{ erg s}^{-1}$.

Using our own fitting value for the FWHM, from which the resultant black hole mass is $7.85 \times 10^7 M_{\odot}$, the Eddington ratio for RX J0136.9-3510 is as high as $\sim 2.7!$ Moreover, if we adopt the lower estimated black hole mass which is $1.3 \times 10^7 M_{\odot}$, then the normalization of `diskpn` is 80, and the resultant disk temperature rises to 31 eV. The UV region is then dominated by disk emission, though the Comptonisation still is required to model the soft X-ray excess. This gives a bolometric flux of $8.8 \times 10^{-11} \text{ ergs s}^{-1} \text{ cm}^{-2}$, giving an even higher Eddington ratio of 13.2! This is the highest known Eddington ratio for an AGN (Vasudevan & Fabian 2009; Shen et al. 2008). Thus modelling the spectral energy distribution with the two extreme mass estimates gives a range for the Eddington ratio of RX J0136.9-3510 of 2.7-13.2. Even without models, simply integrating the observed spectrum using a straight line to connect the UV and soft X-ray data gives an Eddington ratio of ~ 1 for the highest black hole mass, making this a robustly super-Eddington source.

¹ <http://heasarc.gsfc.nasa.gov/cgi-bin/Tools/w3nh/w3nh.pl>

6 SUMMARY AND CONCLUSION

In this paper we report that RX J0136.9-3510 is the only well observed, X-ray bright, variable AGN which has a similar energy dependence to its X-ray variability as the so far unique QPO AGN, RE J1034+396. Its Eddington ratio is similarly high, around 3, although its larger mass means any QPO is undetectable in our data. Its broad band SED is also remarkably similar to that of RE J1034+396, being well modelled by a low temperature, optically thick Comptonisation of the accretion disc spectrum, plus a tail extending to higher energies. Spectra such as this have also been fit by “slim” disc models (Abramowicz, Kato & Matsumoto 1989), where the accretion rate is so high that radiation cannot easily escape vertically before it is carried radially (advected) along with the flow (Puchnarewicz et al. 2001; Wang & Netzer 2003). However, simple slim disc models do not fit the curvature of the soft X-ray spectra as well as Comptonisation (Middleton et al. 2009), although more complex models of slim discs do include such scattering in the disc atmosphere (e.g. Kawaguchi 2003).

Low temperature, optically thick Comptonisation is also occasionally seen in the stellar mass black hole binary systems, for example in the most extreme mass accretion rate spectra of GRS 1915+105 (Middleton et al. 2006; Middleton et al. 2009). Recent studies of spectra of the Ultra-Luminous X-ray sources also indicates that these are well modelled by such material (Gladstone, Roberts & Done 2009). This evidence suggests that there is indeed a distinct spectral state which can only be attained by super Eddington flows (Gladstone, Roberts & Done 2009). Future long duration X-ray observations of AGN should reveal additional examples, and objects with low black hole masses are potential QPO candidates.

ACKNOWLEDGEMENTS

We acknowledge D. Grupe for permission to use the optical data. C. C. Jin acknowledges financial support through Durham Doctoral Fellowship.

REFERENCES

Abramowicz M. A., Kato S., Matsumoto R., 1989, PASJ, 41, 1215
 Bian W., Hu C., Gu Q., Wang J., 2008, MNRAS, 390, 752
 Boller Th., Brandt W. N., Fink H., 1996, A&A, 305, 53
 Boroson T. A., 2002, ApJ, 565, 78
 Brandt W. N., Mathur S., Elvis M., 1997, MNRAS, 285, L25
 Casebeer D. A., Leighly K. M., Baron E., 2006, ApJ, 637, 157
 Crummy J., Fabian A. C., Gallo L., Ross R. R., 2006, ApJ, 365, 1067
 Done C., Ward M. J., Fabian A. C., Kunieda H., Tsuruta S., Lawrence A., Smith M.G., Wamsteker W., 1990, MNRAS, 243, 713
 Edelson R., Vaughan S., Warwick R., Puchnarewicz E., George I., 1999, MNRAS, 307, 91
 Fabian A. C., Miniutti G., Gallo L., Boller Th., Tanaka Y., Vaughan S., Ross R. R., 2004, MNRAS, 353, 1071

Gebhardt K. et al., 2000, ApJ, 539, L13
 Gierliński M., Done C., 2006, MNRAS, 371, L16
 Gierliński M., Middleton M., Ward M., Done C., 2008, Nature, 455, 369
 Ghosh K. K., Swartz D. A., Tennant A. F., Wu J., Ramsey B., 2004, ApJ, 607, L111
 Gladstone J., Roberts T., Done C., MNRAS, submitted
 Goodrich R. W., 1989, ApJ, 342, 224
 Grupe D. 1996, Ph.D. Thesis, Univ. Göttingen
 Grupe D., Beuermann K., Mannheim K., Thomas H. C., 1999, A&A, 350, 805
 Kawaguchi T., 2003, ApJ, 593, 69
 Kuraskiewicz J., Wilkes B. J., Czerny B., Mathur S., 2000, ApJ, 542, 692
 Larsson J., Miniutti G., Fabian A. C., Miller J. M., Reynolds C. S., Ponti G., 2008, MNRAS, 384, 1316
 Leighly K. M., 1999, ApJS, 125, 297
 Leighly K. M., 1999, ApJS, 125, 317
 Magorrian J. et al., 1998, ApJ, 115, 2285
 Mathur S., 2000, MNRAS, 314, L17
 Middleton M., Done C., Gierliński M., Davis S. W., 2006, MNRAS, 373, 1004
 Middleton M., Done C., Gierliński M., 2007, MNRAS, 381, 1426
 Middleton M., Done C., Ward M., Gierliński M., Schurch N., 2009, MNRAS submitted (arXiv:0807.4847v1)
 Morgan E. H., Remillard R. A., Greiner J., 1997, ApJ, 482, 993
 Mullaney J. R., Ward M. J., 2008, MNRAS, 385, 53
 Osterbrock D. E., Pogge R. W., 1985, ApJ, 297, 166
 Petrucci P. O. et al., 2007, A&A, 470, 889
 Ponti G., Miniutti G., Cappi M., Maraschi L., Fabian A. C., Iwasawa K., 2006, MNRAS, 368, 903
 Pounds K. A., Done C., Osborne J. P., 1995, MNRAS, 277, L5
 Puchnarewicz E. M. et al., 1992, MNRAS, 256, 589
 Puchnarewicz E. M., Mason K. O., Siemiginowska A., Pounds, K. A., 1995, MNRAS, 276, 20
 Puchnarewicz E. M., Mason K. O., Siemiginowska A., Fruscione A., Comastri A., Fiore F., Cagnoni I., 2001, ApJ, 550, 644
 Remillard R. A., McClintock J. E., 2006, ARAA, 44, 49
 Shen Y., Greene J. E., Strauss M. A., Richards G. T., Schneider D. P., 2008, ApJ, 680, 169
 Spitzer L. Jr., 1978, JRASC, 72, 349
 Vasudevan R. V., Fabian A. C., 2009, MNRAS, 392, 1124
 Vaughan S., Edelson R., Warwick R. S., Uttley P., 2003, MNRAS, 345, 1271
 Vaughan S., Fabian A. C., 2004, MNRAS, 348, 1415
 Vaughan S., 2005, A&A, 431, 391
 Véron-Cetty M., P., Véron P., Goncalves A. C., 2001, A&A, 372, 730
 Wang J.-M., Netzer H., 2003, A&A, 398, 927
 Wills B. J., Laor, A., Brotherton M. S., Wills, D., Wilkes, B. J., Ferland, G. J., Shang Z., 1999, ApJ, 515, L53
 Winter L. M., Mushotzky R. F., Reynolds C. S., Tueller J., 2009, ApJ, 690, 1322
 Woo Jong-hak, Urry C. M., 2002, ApJ, 579, 530